

See discussions, stats, and author profiles for this publication at: <https://www.researchgate.net/publication/46402422>

# Synthesis of Graphene Aerogel with High Electrical Conductivity

ARTICLE in JOURNAL OF THE AMERICAN CHEMICAL SOCIETY · OCTOBER 2010

Impact Factor: 12.11 · DOI: 10.1021/ja1072299 · Source: PubMed

CITATIONS

307

READS

1,173

6 AUTHORS, INCLUDING:



**Marcus A Worsley**

Lawrence Livermore National Laboratory

90 PUBLICATIONS 1,449 CITATIONS

SEE PROFILE



**Tammy Y. Olson**

Lawrence Livermore National Laboratory

18 PUBLICATIONS 1,021 CITATIONS

SEE PROFILE



**Juergen Biener**

Lawrence Livermore National Laboratory

172 PUBLICATIONS 4,908 CITATIONS

SEE PROFILE

## Synthesis of Graphene Aerogel with High Electrical Conductivity

Marcus A. Worsley,\* Peter J. Pauzauskie,<sup>†</sup> Tammy Y. Olson, Juergen Biener, Joe H. Satcher, Jr., and Theodore F. Baumann

*Physical and Life Science Directorate, Lawrence Livermore National Laboratory, 7000 East Avenue, Livermore, California 94550, United States*

Received August 11, 2010; E-mail: [worsley1@llnl.gov](mailto:worsley1@llnl.gov)

**Abstract:** We report the synthesis of ultra-low-density three-dimensional macroassemblies of graphene sheets that exhibit high electrical conductivities and large internal surface areas. These materials are prepared as monolithic solids from suspensions of single-layer graphene oxide in which organic sol–gel chemistry is used to cross-link the individual sheets. The resulting gels are supercritically dried and then thermally reduced to yield graphene aerogels with densities approaching 10 mg/cm<sup>3</sup>. In contrast to methods that utilize physical cross-links between GO, this approach provides covalent carbon bonding between the graphene sheets. These graphene aerogels exhibit an improvement in bulk electrical conductivity of more than 2 orders of magnitude ( $\sim 1 \times 10^2$  S/m) compared to graphene assemblies with physical cross-links alone ( $\sim 5 \times 10^{-1}$  S/m). The graphene aerogels also possess large surface areas (584 m<sup>2</sup>/g) and pore volumes (2.96 cm<sup>3</sup>/g), making these materials viable candidates for use in energy storage, catalysis, and sensing applications.

Graphene is a two-dimensional (2D) structure of carbon atoms with unique electronic, chemical, and mechanical properties.<sup>1–5</sup> Extensive research has shown the potential of graphene or graphene-based sheets to impact a wide range of technologies including energy storage,<sup>6–10</sup> catalysis,<sup>11,12</sup> sensing,<sup>13–15</sup> and composites.<sup>16–20</sup> Developing three-dimensional (3D) structures with this extraordinary nanomaterial would further expand its significance both in the number of applications and in the manufacturability of devices. However, literature on the assembly of 3D graphene structures is limited.<sup>12,20–24</sup> Typically, previous reports relied on the high stability of graphene oxide (GO) suspensions to assemble an initial GO macrostructure, which was then thermally reduced to yield the 3D graphene network. These reports indicated that physical cross-links (e.g., van der Waals forces) hold the 3D graphene networks together, and, as a result, bulk electrical conductivities of these assemblies only reached approximately  $5 \times 10^{-1}$  S/m.<sup>23</sup> Even when metal cross-links were used between graphene sheets instead of weak physical bonds, electrical conductivities of only  $2.5 \times 10^{-1}$  S/m were reached.<sup>12</sup> These numbers are several orders of magnitude below the conductivity reported for graphene sheets ( $\sim 8 \times 10^3$  S/m) produced by thermal reduction of GO.<sup>25</sup> Clearly, substantial research is needed to realize the full potential of 3D graphene macroassemblies.

In this Communication, we present a unique method for producing ultra-low-density graphene aerogels with high electrical conductivities and large surface areas. A key aspect in fabricating macroassemblies that exhibit such properties was the formation of

junctions between graphene sheets that would both structurally reinforce the assembly and provide conductive interconnections between the individual sheets. The method presented here utilizes carbon to knit together graphene sheets into a macroscopic 3D structure. This approach produces monolithic graphene architectures with low densities (approaching 10 mg/cm<sup>3</sup>) and electrical conductivities more than 2 orders of magnitude greater than those reported for 3D graphene assemblies formed with physical cross-links. Furthermore, the graphene aerogels possess surface areas on par with those reported for very high quality 2D graphene sheets.<sup>25</sup>

We recently reported the synthesis of carbon nanotube (CNT) aerogels that exhibited high electrical conductivity and robust mechanical properties.<sup>26</sup> The CNT aerogels were shown to be the stiffest low-density solid reported and were also highly elastic. These materials were assembled through the formation of covalent carbon cross-links between CNT bundles using organic sol–gel chemistry. Organic sol chemistry involves the polymerization of organic precursors to form a highly cross-linked organic gel, which can then be dried and pyrolyzed to form a carbon aerogel.<sup>27</sup> When the organic precursors were added to a suspension of CNTs, polymerization occurred primarily on the CNTs, both coating the bundles and forming junctions between adjacent bundles. Upon drying and pyrolysis, the organic coating and junctions were converted to carbon, yielding the CNT aerogel. The graphene aerogels presented here were fabricated using a similar approach. In this case, however, GO was used to prepare the initial suspension, while carbonization of the organic cross-links and thermal reduction of the GO to graphene occurred simultaneously during pyrolysis. Graphene aerogel synthesis was carried out by sol–gel polymerization of resorcinol (R) and formaldehyde (F) with sodium carbonate as a catalyst (C) in an aqueous suspension of GO. The GO was produced by the Hummers method,<sup>28</sup> and the suspension was prepared by ultrasonication. The molar ratio of R:F was 1:2, the reactant concentration in the starting mixture was 4 wt % RF solids, and the concentration of GO in suspension was 1 wt %. The molar ratio of R:C was 200:1. The sol–gel mixture was cured in sealed glass vials at 85 °C. After gelation, the wet GO–RF gels were removed from the glass vials and washed in acetone to remove water from the pores. Supercritical CO<sub>2</sub> was used to dry the GO–RF gels, and pyrolysis at 1050 °C under nitrogen yielded the final graphene aerogel. Energy-dispersive X-ray analysis confirmed the successful reduction of the GO–RF gel, showing a drop in atomic oxygen from 17% to 1% (Figure S1, Supporting Information).

Field-emission scanning electron micrographs (FE-SEM) of the graphene aerogel show a 3D network of randomly oriented sheet-like structures (Figure 1a,b) similar to those seen in previous reports of thermally reduced GO.<sup>10</sup> The lateral dimensions of the sheets ranged from hundreds of nanometers to several micrometers. Within the assembly, the sheets are thin enough to be transparent to the

<sup>†</sup> Current address: Department of Materials Science & Engineering, University of Washington, Seattle, WA 98195-2120.

electron beam. Transmission electron micrographs (TEM) reveal a wrinkled paper-like texture to the sheets (Figure 1c,d), again consistent with previous reports.<sup>29</sup> It is important to note that, in both the FE-SEM and TEM images, we do not observe carbon nanoparticles from the RF polymer decorating the surfaces of the graphene sheets, despite the fact that over half of the weight in the reduced GO–RF structure can be attributed to carbon from the RF polymer (56 wt % from RF vs 44 wt % from GO). This is in sharp contrast to what occurs in materials prepared at higher RF:GO ratios (Figure S2, Supporting Information) or in CNT aerogels, where the carbonized RF is clearly distinguishable.<sup>30</sup> This observation suggests that the carbon junctions are effectively incorporated into the extended graphene framework. When the organic precursors are added at sufficiently low concentrations to the GO suspension, polymerization likely occurs preferentially at the oxygen functionalities of the GO to form covalent interconnections between individual sheets. Simultaneous carbonization of the RF junctions and thermal reduction of the GO apparently blends these two materials into a single structure, yielding the graphene macroassembly.

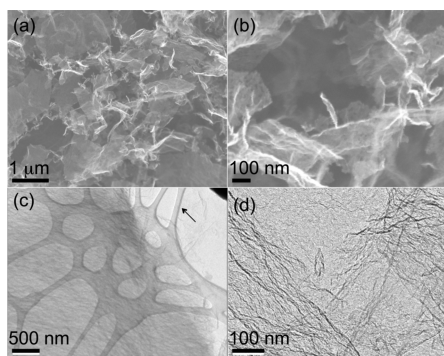


**Figure 1.** FE-SEM of the graphene aerogel at low (a) and high (b) magnification. TEM of the graphene aerogel at low (c) and high (d) magnification. Black arrow denotes holey carbon on TEM grid.

The Type IV nitrogen adsorption/desorption isotherm for the graphene aerogel indicates that the material is mesoporous. The Type 3 hysteresis loop (IUPAC classification) at high relative pressure is typically associated with adsorption within aggregates of plate-like particles, consistent with the microstructure observed by FE-SEM and TEM. The pore size distribution for the graphene aerogel, as determined by the BJH method, shows that much of the pore volume (2.96 cm<sup>3</sup>/g) lies in the 10–100 nm range, with a peak pore diameter of 13 nm (Figure 2b). The BET surface area for the graphene aerogel was 584 m<sup>2</sup>/g. This value is less than the theoretical surface area for a single graphene sheet (>2600 m<sup>2</sup>/g),<sup>31</sup> likely due to layering or overlapping of graphene sheets within the assembly. Nevertheless, the measured surface area is on par with those reported for high-quality graphene sheets prepared via hydrogen arc discharge<sup>25</sup> and is more than 2 times greater than that of the CNT aerogel.<sup>30</sup>

Bulk electrical conductivity of the graphene aerogel was determined via the four-probe method. Current (100 mA) was passed through metal electrodes attached to either end of the graphene aerogel monolith, and the voltage drop was measured over distances of 3–6 mm along the aerogel. The bulk electrical conductivity of the graphene aerogel was determined to be 87 S/m, more than 2 orders of magnitude greater than those reported for macroscopic 3D graphene networks prepared with physical cross-links.<sup>12,23</sup> We believe this extraordinarily high conductivity is due to a large reduction in resistance at the junctions between

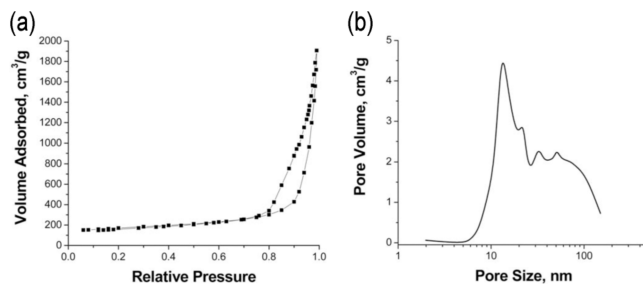


**Figure 2.** Nitrogen adsorption/desorption isotherm (a) and pore size distribution (b) for the graphene aerogel.

graphene sheets compared to those in the physically bonded networks. A detailed discussion of the nature of the carbon junction will be presented in a forthcoming paper.

In conclusion, we prepared a macroscopic 3D graphene assembly with high electrical conductivity and large surface area. Our approach used an organic binder that could be reduced concurrently with the GO to produce carbon cross-links in the graphene network that were virtually indistinguishable from those in the graphene sheets. Due to the high surface area, mesoporosity, and conductivity of these 3D graphene assemblies, they have potential in a number of technologies for use as supercapacitors, batteries, catalysis, and sensors.

**Acknowledgment.** This work was performed under the auspices of the U.S. Department of Energy by Lawrence Livermore National Laboratory under Contract DE-AC52-07NA27344 and funded by the DOE Office of Energy Efficiency and Renewable Energy.

**Supporting Information Available:** Synthesis and characterization methods, EDX spectra, TEM, and FE-SEM figures. This material is available free of charge via the Internet at <http://pubs.acs.org>.

## References

- (1) Geim, A. K.; Novoselov, K. S. *Nat. Mater.* **2007**, *6*, 183.
- (2) Gomez-Navarro, C.; Weitz, R. T.; Bittner, A. M.; Scolari, M.; Mews, A.; Burghard, M.; Kern, K. *Nano Lett.* **2007**, *7*, 3499.
- (3) Lee, C.; Wei, X.; Kysar, J. W.; Hone, J. *Science* **2008**, *321*, 385.
- (4) Li, X. L.; Zhang, G. Y.; Bai, X. D.; Sun, X. M.; Wang, X. R.; Wang, E.; Dai, H. J. *Nature Nanotechnol.* **2008**, *3*, 538.
- (5) Novoselov, K. S.; Geim, A. K.; Morozov, S. V.; Jiang, D.; Zhang, Y.; Dubonos, S. V.; Grigorieva, I. V.; Firsov, A. A. *Science* **2004**, *306*, 666.
- (6) Eda, G.; Fanchini, G.; Chhowalla, M. *Nature Nanotechnol.* **2008**, *3*, 270.
- (7) Vivekchand, S. R. C.; Rout, C. S.; Subrahmanyam, K. S.; Govindaraj, A.; Rao, C. N. R. *J. Chem. Sci.* **2008**, *120*, 9.
- (8) Vollmer, a.; Feng, X. L.; Wang, X.; Zhi, L. J.; Mullen, K.; Koch, N.; Rabe, J. P. *Appl. Phys. a—Mater. Sci. Process.* **2009**, *94*, 1.
- (9) Wang, X.; Zhi, L. J.; Mullen, K. *Nano Lett.* **2008**, *8*, 323.
- (10) Yoo, E.; Kim, J.; Hosono, E.; Zhou, H.; Kudo, T.; Honma, I. *Nano Lett.* **2008**, *8*, 2277.
- (11) Sutter, P. W.; Flege, J. I.; Sutter, E. A. *Nat. Mater.* **2008**, *7*, 406.
- (12) Tang, Z. H.; Shen, S. L.; Zhuang, J.; Wang, X. *Angew. Chem., Int. Ed.* **2010**, *49*, 4603.
- (13) Fowler, J. D.; Allen, M. J.; Tung, V. C.; Yang, Y.; Kaner, R. B.; Weiller, B. H. *ACS Nano* **2009**, *3*, 301.
- (14) Schedin, F.; Geim, A. K.; Morozov, S. V.; Hill, E. W.; Blake, P.; Katsnelson, M. I.; Novoselov, K. S. *Nat. Mater.* **2007**, *6*, 652.
- (15) Shao, Y.; Wang, J.; Wu, H.; Liu, J.; Aksay, I. A.; Lin, Y. *Electroanalysis* **2010**, *22*, 1027.
- (16) Ramanathan, T.; Abdala, A. A.; Stankovich, S.; Dikin, D. A.; Herrera-Alonso, M.; Piner, R. D.; Adamson, D. H.; Schniepp, H. C.; Chen, X.; Ruoff, R. S.; Nguyen, S. T.; Aksay, I. A.; Prud'homme, R. K.; Brinson, L. C. *Nature Nanotechnol.* **2008**, *3*, 327.
- (17) Stankovich, S.; Dikin, D. A.; Dommett, G. H. B.; Kohlhaas, K. M.; Zimney, E. J.; Stach, E. A.; Piner, R. D.; Nguyen, S. T.; Ruoff, R. S. *Nature* **2006**, *442*, 282.
- (18) Verdejo, R.; Barroso-Bujans, F.; Rodriguez-Perez, M. A.; de Saja, J. A.; Lopez-Manchado, M. A. *J. Mater. Chem.* **2008**, *18*, 2221.
- (19) Cote, L. J.; Cruz-Silva, R.; Huang, J. *J. Am. Chem. Soc.* **2009**, *131*, 11027.
- (20) Vickery, J. L.; Patil, A. J.; Mann, S. *Adv. Mater.* **2009**, *21*, 2180.
- (21) Liu, F.; Seo, T. S. *Adv. Funct. Mater.* **2010**, *20*, 1930.
- (22) Wang, J.; Ellsworth, M. *ECS Trans.* **2009**, *19*, 241.
- (23) Xu, Y.; Sheng, K.; Li, C.; Shi, G. *ACS Nano* **2010**, *4*, 4324.

- (24) Zu, S. Z.; Han, B. H. *J. Phys. Chem. C* **2009**, *113*, 13651.
- (25) Wu, Z.-S.; Ren, W.; Gao, L.; Zhao, J.; Chen, Z.; Liu, B.; Tang, D.; Yu, B.; Jiang, C.; Cheng, H.-M. *ACS Nano* **2009**, *3*, 411.
- (26) Worsley, M. A.; Kucheyev, S. O.; Satcher, J. H.; Hamza, A. V.; Baumann, T. F. *Appl. Phys. Lett.* **2009**, *94*, 073115.
- (27) Pekala, R. W.; Kong, F. M. *Abstracts of Papers*, 197th National Meeting; American Chemical Society: Washington, DC, 1989; p 113.
- (28) Hummers, W.; Offman, R. *J. Am. Chem. Soc.* **1958**, *80*, 1339.
- (29) McAllister, M. J.; Li, J. L.; Adamson, D. H.; Schniepp, H. C.; Abdala, A. A.; Liu, J.; Herrera-Alonso, M.; Milius, D. L.; Car, R.; Prud'homme, R. K.; Aksay, I. A. *Chem. Mater.* **2007**, *19*, 4396.
- (30) Worsley, M. A.; Pauzauskie, P. J.; Kucheyev, S. O.; Zaug, J. M.; Hamza, A. V.; Satcher, J. H.; Baumann, T. F. *Acta Mater.* **2009**, *57*, 5131.
- (31) Peigney, A.; Laurent, C.; Flahaut, E.; Bacsa, R. R.; Rousset, A. *Carbon* **2001**, *39*, 507.

JA1072299